NJC

New Journal of Chemistry

A journal for new directions in chemistry

Accepted Manuscript

This article can be cited before page numbers have been issued, to do this please use: P. M. Zagórski, P. Tokarz, B. Gostynski and P. Tokarz, *New J. Chem.*, 2020, DOI: 10.1039/D0NJ00963F.

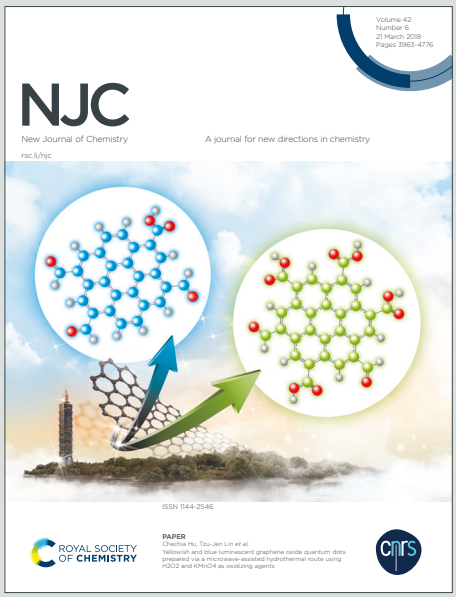

This is an Accepted Manuscript, which has been through the Royal Society of Chemistry peer review process and has been accepted for publication.

Accepted Manuscripts are published online shortly after acceptance, before technical editing, formatting and proof reading. Using this free service, authors can make their results available to the community, in citable form, before we publish the edited article. We will replace this Accepted Manuscript with the edited and formatted Advance Article as soon as it is available.

You can find more information about Accepted Manuscripts in the Information for Authors.

Please note that technical editing may introduce minor changes to the text and/or graphics, which may alter content. The journal's standard Terms & Conditions and the Ethical guidelines still apply. In no event shall the Royal Society of Chemistry be held responsible for any errors or omissions in this Accepted Manuscript or any consequences arising from the use of any information it contains.

Experimental and computational studies on the formation and biological properties of the simplest polyfluoroalkyl phosphonates

Piotr M. Zagórski[1], Paulina Tokarz[2], Bartłomiej Gostyński[3], Paweł Tokarz[4]

[1]University of Lodz, Faculty of Chemistry, Department of Organic Chemistry, Tamka 12, 91-403 Lodz

[2]University of Lodz, Faculty of Biology and Environmental Protection, Department of Molecular Genetics, Pomorska 141/143, 90-236 Lodz, Poland

[3]Centre of Molecular and Macromolecular Studies, Polish Academy of Sciences, Sienkiewicza 112, Lodz 90-363, Poland

[4]University of Lodz, Faculty of Chemistry, Department of Organic Chemistry, Molecular Spectroscopy Laboratory, Tamka 12, 91-403 Lodz

Abstract

A representative set of the simplest dialkyl polyfluoroalkylphosphonates was *in silico* profiled against their absorption, distribution, metabolism, and excretion with the use of the SwissADME tool. Promising results of the screening led us to attempt to synthesize the title compounds for further biological investigations. Detailed experimental and quantum-theoretical (DFT) investigations were performed to reveal that the studied compounds could not be obtained through the standard Michaelis-Arbuzov or Michaelis-Becker reactions. Kinetic studies showed that the trimethyl phosphite undergoes a reaction with 1,1,1-trifluoro-2-iodoethane at several orders of magnitude slower than a side reaction. The difficulty was overcome by developing a simple three-step synthesis path that involves only readily available substrates. The newly synthesized substances were tested against several cell lines. The *in vitro* research revealed that both dimethyl and diethyl (2,2,3,3,3-pentafluoropropyl)phosphonate exhibited toxicity towards the glioblastoma cells (U-87 MG) at a considerably lower concentration than known chemotherapeutics.

Keywords: polyfluoroalkyl phosphonates, toxicity, glioblastoma, ADME, kinetics

Corresponding author: Paweł Tokarz; pawel.tokarz@chemia.uni.lodz.pl; +48 42 635 58 12

This work is dedicated to the memory of Professor Jarosław Lewkowski, our colleague, teacher and friend.

Additional data are available in the Electronic supporting information

View Article Online
DOI: 10.1039/D0NJ00963F

1. Introduction

The interest in a synthesis of fluorinated and perfluoroalkylated compounds is a still-growing trend in chemistry. This is motivated by the fact that fluorine atoms notably change the physicochemical properties of organic molecules, including their biological activity. Particularly, perfluoroalkylated chains increase the lipophilicity and interactions with several cellular structures.[1] For these reasons trifluoromethyl group, which constitutes the smallest polyfluorinated moiety that can be incorporated into a molecule in numerous ways, is commonly found in medicines.[2-7] Equally interesting are biochemical characteristics of the phosphonic moiety. Phosphonates occur naturally in numerous structures of living organisms and play an important role in several biochemical pathways.[8] Specifically, they can be recognized by enzymes related to phosphorylation/dephosphorylation processes and support trans-membrane transport, particularly anionic chemical delivery system (aCDS), which is used to deliver molecules to nerve cells.[9, 10] This led us to a question of possible biological activity of a molecule with both polyfluoroalkyl and phosphonic moieties combined with merely no other functional group. Surprisingly, the literature study returned virtually no data related to any biological activity of such structures – a strikingly peculiar gap when the molecular simplicity of the compounds is considered.

Not only the references to the bioactivity but also the synthesis of the simplest possible polyfluoroalkyl phosphonates are limited. For the first time the dimethyl (2,2,2-trifluoroethyl)phosphonate was obtained by the hydrolysis of dimethyl pentafluoroisopropenylphosphonate with only 10% yield.[11] The first practically useful method of the synthesis of the target compounds was developed in 2016 by the Gouverneur group.[12] The method exploits 2,2,2-trifluoro-1-diazoethane which has been considered possibly explosive.[13] Recently, several dialkyl (2,2,2-trifluoroethyl)phosphonates have been prepared from 1,1-dichloro-2,2,2-trifluoroethane or trifluoroacetaldehyde *N*-tosylhydrazone utilizing copper-mediated synthesis.[14, 15] While both, 2,2,2-trifluoro-1-diazoethane and 1,1-dichloro-2,2,2-trifluoroethane are readily available from commercial sources they remain rather expensive starting materials. Moreover, their homologs with longer fluorinated chains are less accessible and even more expensive. Thus, we faced a problem of the accessibility of the desired compounds.

Throughout the article, the dialkyl polyfluoroalkyl phosphonates of formula $C_xF_y(CH_2)_nP(O)(OR)_2$ (x=1,2, y=2x+1, n=1,2,3, R=Me, Et) will be referred to as **ZOT$_y$-n-R**, according to the naming convention used in our research project (**Scheme 1**).

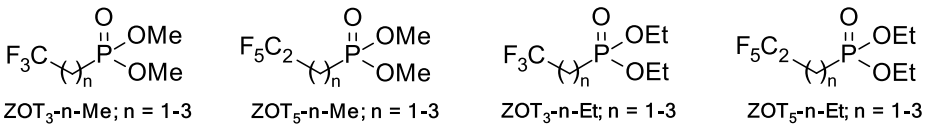

Scheme 1. *The studied compounds.*

2. Results and discussion

2.1. ADME profiling

Due to a lack of biological data related to the **ZOTs**, we decided to perform *in silico* screening, concerning the plausible absorption, distribution, metabolism, and excretion (ADME)

View Article Online
DOI: 10.1039/D0NJ00963F

processes descriptors. The analysis was performed using the SwissADME – a free-to-use tool provided online by the Swiss Institute for Bioinformatics.[16, 17]

The tool provides results of bioinformatic calculations of several molecular descriptors associated with physicochemical properties that strongly impact the biochemical properties of a substance, including lipophilicity, size, polarity, insolubility, insaturation, and flexibility. We tested trifluorinated and pentafluorinated phosphonates. Lipophilicity was calculated as XLOGP3, an atomistic method including corrective factors and knowledge-based library.[18] For polarity, the tool uses a topological polar surface, an additive model based on contributions of separate atoms considered polar.[19] Solubility was predicted by the use of the ESOL descriptor (Estimated SOLubility).[20] Flexibility is simply expressed as the number of rotatable bonds. The compound is considered promising if its descriptor values lie in the subspace of the physicochemical properties suitable for bioavailability. Graphically, the bioavailability subspace can be represented by an area on a six-axis plot on which the most critical parameters are taken into account. It is clearly visible that considered fluorinated phosphonates fit perfectly into the desired subspace (**Fig. 1**).

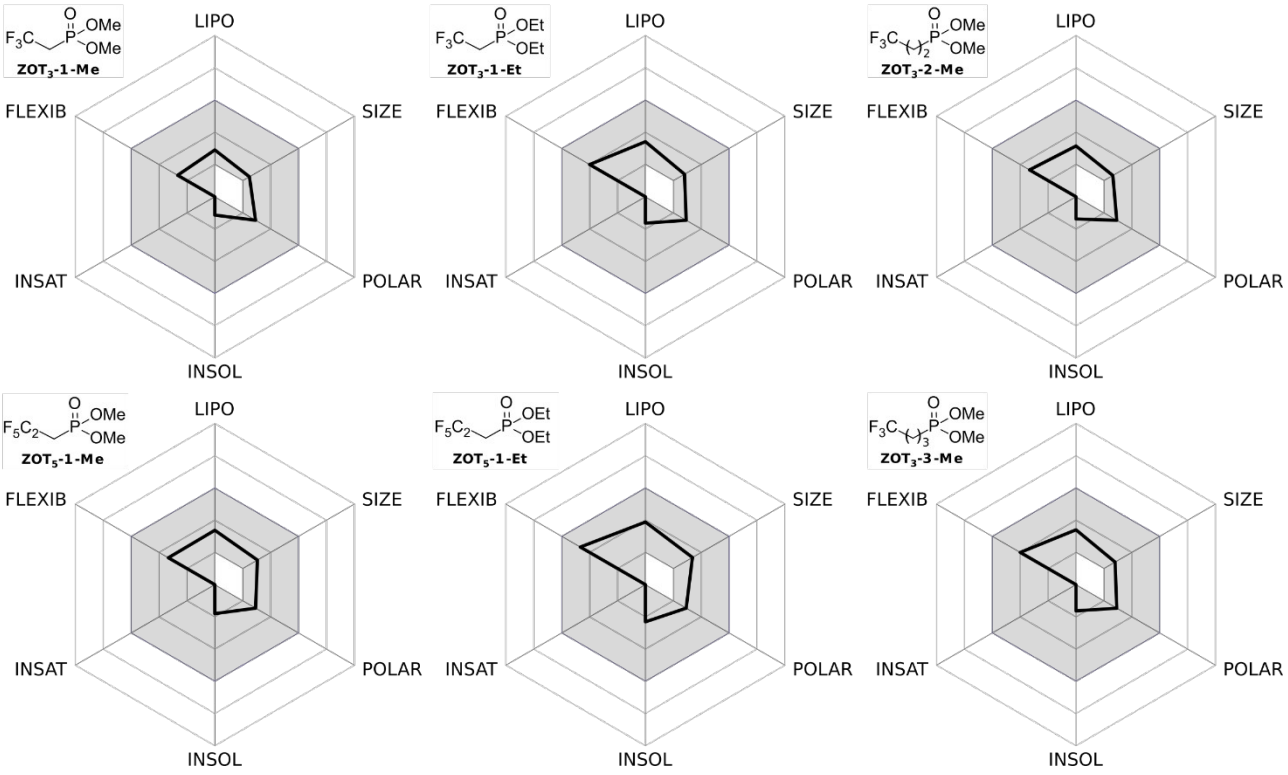

Figure 1. *Radar plots of the main ADME parameters: lipophilicity (XLOGP3), molecular size, polarity (TPSA), insolubility (*log *S(ESOL)), insaturation (fraction of the* sp^3 *carbons) and flexibility (number of rotatable bonds). The grey area represents the suitable physicochemical subspace for oral bioavailability according to the literature.*[16] *Consult the main text (Section 2.1) and the corresponding Table 1 for further details and values.*

The selected descriptors critical for predicting the pharmacokinetics and the druglikeness of the compounds have been analyzed and summarized in **Tab. 1**. All tested **ZOTs** showed high gastrointestinal(GI) absorption and blood-brain barrier (BBB) permeability.[21] Additionally, all tested **ZOTs** were estimated to be non-substrates of p-glycoprotein (P-gp) and non-inhibitors of a given cytochrome P450 (CYP) isomers using algorithm design in SwissADME.[17] P-gp is a key member of ATP-binding cassette transporters, which protects the central nervous system

(CNS) from xenobiotics and is associated with multidrug-resistance (MDR) in cancers. CYP isomers are the major executors of xenobiotics biotransformation and the alteration of their activity can result in harmful drug-drug interactions due to the production of metabolites with the pharmacological and toxicological profiles different from the original drug. Since **ZOTs** are predicted to be inert to P-gp and CYP isomers it can be expected that **ZOTs** should be resistant to P-gp-mediated drug elimination and its intake should be safe in the respect of drug metabolism.

The Lipinski[22], Ghose[23], Veber[24], Egan[25], and Muegge[26] rules were applied to evaluate druglikeness to predict whether a compound is likely to be orally bioavailable. The number of violations to these rules is documented in **Tab. 1**. All analyzed compounds lie within the range of all the parameters of the Lipinski, Veber, and Egan rules and demonstrated the bioavailability score of 0.55. According to the evaluation, **ZOT$_3$-1-Me**, **ZOT$_5$-1-Me**, **ZOT$_3$-2-Me** lie within the close agreement with the Ghose and Muegge rules while the rest of the compounds abide with the criteria.

Table 1. *The main results of the ADME analysis of ZOTs. The minimum and maximum values describe the subspace for oral bioavailability. For a detailed description consult the main text (Section 2.1). The full set of data returned by SwissADME is available in the Supplementary Material file.*

Molecule	ZOT$_3$-1-Me	ZOT$_3$-1-Et	ZOT$_5$-1-Me	ZOT$_5$-1-Et	ZOT$_3$-2-Me	ZOT$_3$-3-Me	Min	Max
MW	192,07	220,13	242,08	270,13	206,1	220,13	150	500
Insaturation	1	1	1	1	1	1	0,25	1,00
Rotatable bonds	4	6	5	7	5	6	0	9
Polarity TPSA	45,34	45,34	45,34	45,34	45,34	45,34	20	130
Lipophilicity XLOGP3	0,59	1,32	1,26	1,99	0,94	1,3	0,70	50
Insolubility ESOL Log S	-1,14	-1,64	-1,8	-2,31	-1,38	-1,63	-6	0
GI absorption	High	High	High	High	High	High		
BBB permeant	Yes	Yes	Yes	Yes	Yes	Yes		
P-gp substrate	No	No	No	No	No	No		
CYP1A2 inhibitor	No	No	No	No	No	No		
CYP2C19 inhibitor	No	No	No	No	No	No		
CYP2C9 inhibitor	No	No	No	No	No	No		
CYP2D6 inhibitor	No	No	No	No	No	No		
CYP3A4 inhibitor	No	No	No	No	No	No		
Lipinski #violations	0	0	0	0	0	0		
Ghose #violations	2	0	1	0	1	0		
Veber #violations	0	0	0	0	0	0		
Egan #violations	0	0	0	0	0	0		
Muegge #violations	2	0	0	0	0	0		
Bioavailability Score	0,55	0,55	0,55	0,55	0,55	0,55		
PAINS #alerts	0	0	0	0	0	0		
Leadlikeness #violations	1	1	1	0	1	1		

MW – molecular weight
GI absorption – gastrointestinal absorption
BBB – blood-brain barrier permeability
P-gp – p-glycoprotein

SwissADME performs an analysis of pan assay interference compounds (PAINS)[27] which allow to exclude compounds that give the false-positive response in biological assays from the drug-discovery process. The evaluation of ZOTs returned no warnings with the PAINS filter. All remaining data are available in the supplementary material.

View Article Online
DOI: 10.1039/D0NJ00963F

2.2. Michaelis-Arbuzov reaction kinetics

Promising ADME parameters fully justified the attempts of the synthesis of **ZOTs**. We decided to keep the synthesis as simple as possible exploiting only readily available substrates. This is essential when higher fluorinated homologs are considered. This is why we initially focused on the Michaelis-Arbuzov protocol. The reaction alkyl halide and trialkyl phosphite is a standard method of choice when the synthesis of an alkylphosphonates is desired. Thus, our first attempt to obtain the polyfluoroalkyl phosphonates was to exploit a set of reactions between the appropriate polyfluoroalkyl iodides and trimethyl phosphite (TMP) (**Scheme 2**, **reaction 1**). We expected a formation of minor amounts of **2** as a typical by-product – a result of the side reaction between the trimethyl phosphite and methyl iodide liberated during the main reaction (**Scheme 2**, **reaction 2**). Surprisingly, the ^{1}H and ^{31}P NMR spectra recorded from the reaction mixture did not reveal the formation of the desired fluorinated phosphonate at all. Instead, the only detectable product observed was dimethyl methyl phosphonate (**2**). Regardless of the conditions applied, the only process that took place was the formal rearrangement of the TMP to **2**.

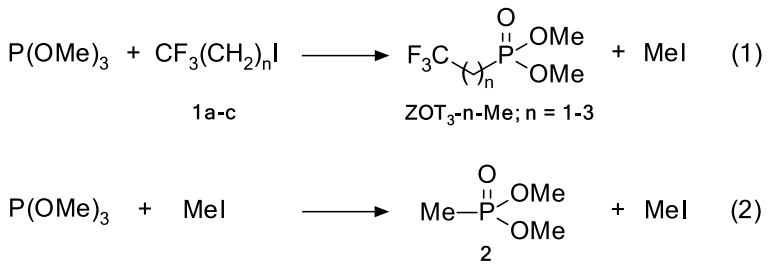

Scheme 2. *The desired Michaelis-Arbuzov reaction (1) and the side-reaction (2) of methyl iodide.*

We hypothesized that reaction 1 is of several orders of magnitude slower than reaction 2 thus the amount of **ZOT** produced is too low for being observed on NMR while the amount of methyl iodide being enough to sustain the rearrangement cycle. Typically, one could simply perform the reaction in an open flask to allow the methyl iodide to leave the system. However, the volatility of the substrate rendered such technique inapplicable. We attempted to verify this hypothesis by kinetic experiments. Since direct measurement of the kinetics of the reaction 1 would be virtually impossible due to an extremally low rate of the process we developed a mathematical model of the reaction system from which the desired parameters could be extracted. The dependency of the concentration of **2** on the reaction time found with aid of the Wolfram Development Platform at Wolfram Cloud[28] follows the formula: (**Eq. 1**):

$$x_{MeP(O)(OMe)_2} = x_{0,P(OMe)_3} \tanh^2\left(t\sqrt{\frac{1}{2}k_1 k_2 x_{CF_3(CH_2)_nI}\, x_{0,P(OMe)_3}}\right) \quad (1)$$

To estimate the reaction rate constants k_1 and k_2 we performed two series of NMR-controlled kinetic experiments. First, the kinetics of the simpler reaction 2 was examined by heating the samples of trimethyl phosphite containing respectively 0, 0.01, 0.02, and 0.04 mole fraction of methyl iodide. The reactions were run at 50 °C and the progress was monitored by ^{31}P and ^{1}H NMR for 16 hours (see the *Experimental* section for technical details).

The initial reaction rate v_0 is linearly proportional to the reaction rate constant k_2 and the concentration of methyl iodide. This is understandable, as methyl iodide can be formally considered a catalyst for the reaction.

$$\frac{v_0}{x_{0,P(OMe)_3}} = k_2 x_{MeI} \quad (2)$$

The value of v_0 for each methyl iodide concentration was estimated from the initial data points as presented in **Fig. 2**. The reaction rate constant calculated by regression was found to equate $k_2 = 7.24 \cdot 10^{-4}$ s^{-1}.

To determine the rate constants k_1 of the reaction 1 for each of three different fluorinated iodides (n=1,2,3) three separate reaction mixtures with trimethyl phosphite were prepared. In each of them, the molar fraction of the fluorinated iodide was equal to $x_{CF_3(CH_2)_nI} = 0.1$ ($x_{0,P(OMe)_3} = 0.9$). The reactions were run at 50 °C and monitored on ^{31}P and ^{1}H NMR.

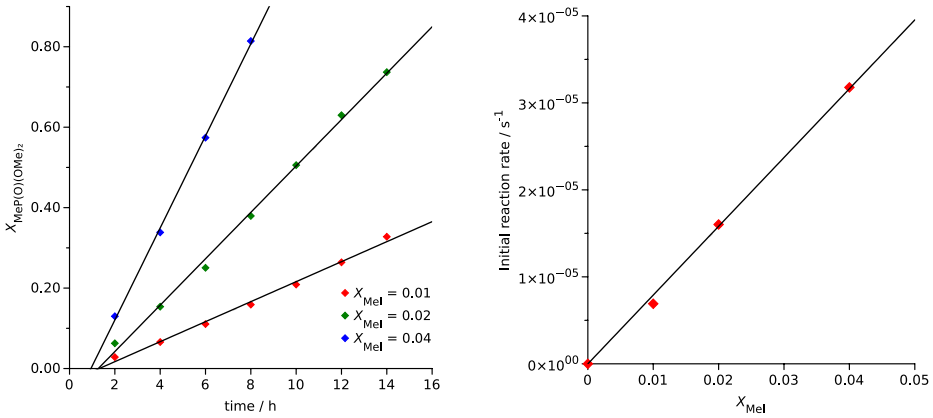

Figure 2. *Left: the concentration of the product of the Michaelis-Arbuzov reaction vs. the reaction time depending on the methyl iodide concentration. Right: dependence of the initial reaction rate vs. the methyl iodide concentration.*

A qualitative examination of the plotted data showed the expected "sigmoid" shape (**Fig. 3**). However, the attempt of fitting the squared hyperbolic tangent function in accordance with **Eq. 1** to the data revealed a significant discrepancy between the theoretical model and the empirical results. As a plausible explanation to this could serve the fact that the theoretical model does not account for the changes of the physical properties, especially dielectric constant and viscosity of the reaction medium throughout the reaction progress (at the beginning the reaction mixture is dominated by the trimethyl phosphite which becomes successively replaced by the phosphonate **2**). The incorporation of the changes of the reaction medium properties into a solvable differential equation system would require unsolicited assumptions that we decided to avoid. However, during the initial stage of the reaction progress, it can be safely assumed that $x_{P(OMe)_3}$ and the dielectric constant remains quasi-constant. In such case the solution to the differential equation system simplifies to becomes quadratic (**Eq. 3**):

$$x_{MeP(O)(OMe)_2} = \frac{1}{2} t k_1 k_2 \left(x_{0,P(OMe)_3}\right)^2 x_{CF_3(CH_2)_nI} \qquad (3)$$

This should be expected, as the initial increase of the concentration of the methyl iodide produced in reaction 1 is linear thus the increase of the concentration of the product of the reaction 2 catalyzed by this iodide must be a quadratic function of the reaction time. After fitting the data from the initial stage of the reaction progress (arbitrarily set to $x_{MeP(O)(OMe)_2} \leq 0.2$) with a quadratic function, the k_2 values for each substrate were easily calculated from the second-order coefficient of the resulting trinomial (**Fig. 3**).

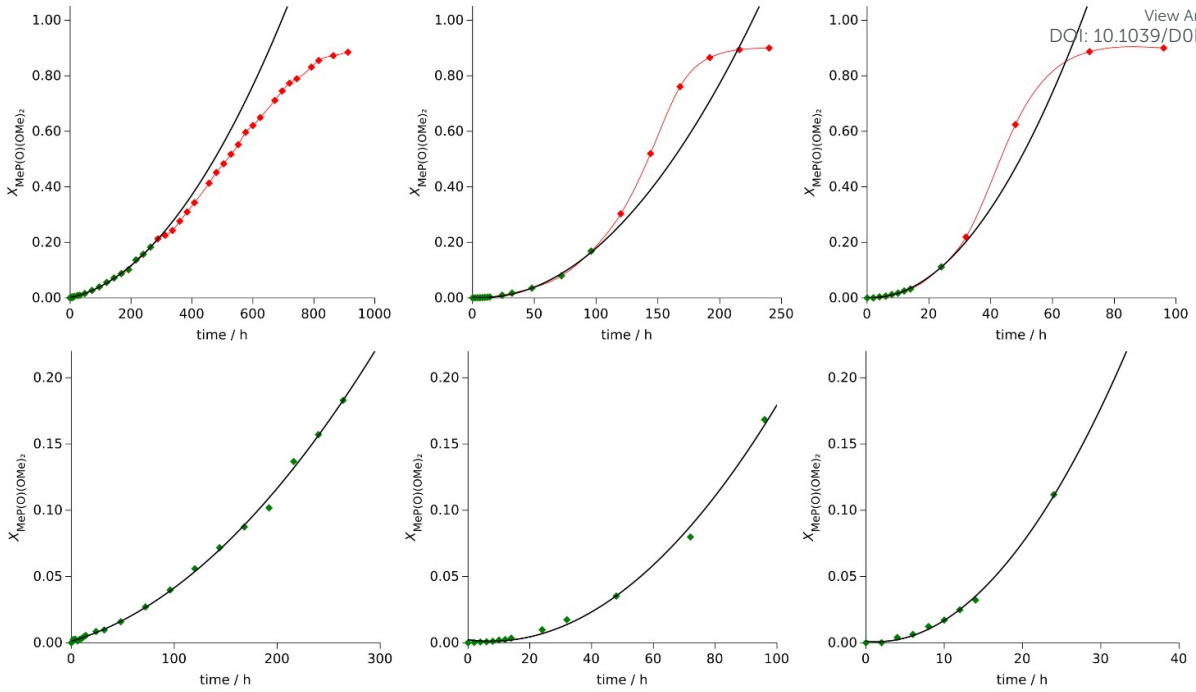

Figure 3. *Reaction progress as measured by the integration of ^{31}P NMR spectra. Top: the full set of data with the data used for fitting marked as green; note the sigmoidal shape of the curve, reassembling the squared hyperbolic tangent, as predicted by* ***Eq. 1****. Bottom: magnified part of the data taken for fitting the quadratic function as predicted by* ***Eq. 3****. Black line – the fitting curve.*

The values of the calculated reaction rate constants are presented in the **Tab. 2**. It is clearly visible that the Arbuzov reaction of the 1,1,1-trifluoro-2-iodoethane is about 350 thousand times slower than the side reaction with the methyl iodide. Even in the case of 1,1,1-trifluoro-4-iodobutane, the main reaction is almost 3000 times slower than the side reaction. Elongation of the linker between the CF_3 group and the iodine atom by one methylene moiety causes the reaction to speed up about ten times.

Table 2. *Reaction rate constants of the Arbuzov reaction for different iodides.*

Substrate	Reaction rate constant / s^{-1}
CH_3I	$7.24 \cdot 10^{-4}$
CF_3CH_2I (**1a**)	$2.06 \cdot 10^{-9}$
$CF_3CH_2CH_2I$ (**1b**)	$2.46 \cdot 10^{-8}$
$CF_3CH_2CH_2CH_2I$ (**1c**)	$2.55 \cdot 10^{-7}$

2.3. Michalis-Becker reaction

To avoid the above described competitive side reaction of methyl iodide liberated from TMP, we attempted to employ the Michaelis-Becker protocol instead. The appropriate anionic phosphonic nucleophile was generated from dimethyl *H*-phosphonate and sodium hydride in DMF solution (**Scheme 3**, **reaction 3**) and treated with an appropriate iodide (**1a-c**) at room temperature (**Scheme 3**, **reaction 4**).

View Article Online
DOI: 10.1039/D0NJ00963F

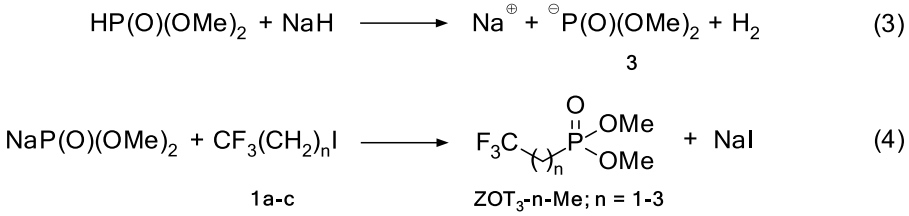

Scheme 3. *Michaelis-Becker synthesis: generation of the phosphite salt (3) and its reaction with the appropriate iodide.*

This approach allowed us to obtain products **ZOT$_3$-2-Me** and **ZOT$_3$-3-Me** with yields of 16% and 62% respectively (**Tab. 3**). However, no traces of **ZOT$_3$-1-Me** have been observed. In all cases, the formation of byproduct **2** was observed. However, its origin is different than in the case of the Michaelis-Arbuzov reaction – it is probably formed in a nucleophilic attack of the anion **3** on the methoxy group from dimethyl *H*-phosphonate (**Scheme 4**). Prolonged reaction time did not affect the yield distribution significantly.

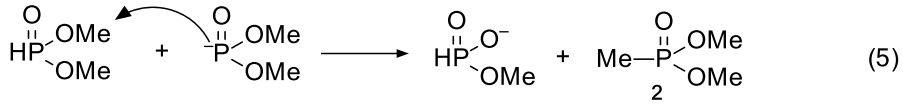

Scheme 4. *The plausible mechanism of the side reaction of the Michaelis-Becker synthesis in which the **2** is formed along with the desired fluorinated phosphonate.*

Table 3. *Yields (isolated) of the Michaelis-Becker reaction for different iodides.*

Substrate	Yield / %
CF_3CH_2I (**1a**)	0
$CF_3CH_2CH_2I$ (**1b**)	16.1
$CF_3CH_2CH_2CH_2I$ (**1c**)	62.2

2.4. Theoretical calculations

Comparing the results obtained from the Michaelis-Becker and Michaelis-Arbuzov reaction it was clearly visible that the proximity of the trifluoromethyl group causes a significant decrease in the reactivity of the electrophilic center in fluorinated iodides.

For a better insight into the molecular course of the substitution, we performed DFT calculations. First, the Michaelis-Becker reaction was chosen for modeling as its mechanism is simpler. All reactions were modeled as solutions in DMF (consult the *Experimental* section for technical details). The overall process was modeled as two separated reactions – formation of the sodium salt and the substitution of the iodide.

The first stage (**Scheme 3**, **reaction 3**) is the same in all cases thus it does not contribute to the observed differences. The reaction runs in an open-system and the newly-created hydrogen gas leaves the medium.

View Article Online
DOI: 10.1039/D0NJ00963F

Table 4. *Energetic contributions of reactions 3-4 in the total reaction referring to reactions occurring in DMF solution (temperature 273.15 K for reaction 3 and 298.15 K for reaction 4).*

Reaction 3	
ΔH / kcal mol^{-1}	ΔG / kcal mol^{-1}
-23.98	-23.07

Reaction 4		
Substrate	ΔH / kcal mol^{-1}	ΔG / kcal mol^{-1}
CF_3CH_2I (**1a**)	-51.12	-49.36
$CF_3CH_2CH_2I$ (**1b**)	-51.41	-49.43
$CF_3CH_2CH_2CH_2I$ (**1c**)	-50.41	-48.06

The second reaction (**Scheme 3**, **reaction 4**) was considered the limiting step thus we discuss it in detail. Free energy changes for n=1,2,3 indicate that in each case the process is thermodynamically preferred (**Tab. 4**), thus differences in the reaction yields may exist due to kinetic factors.

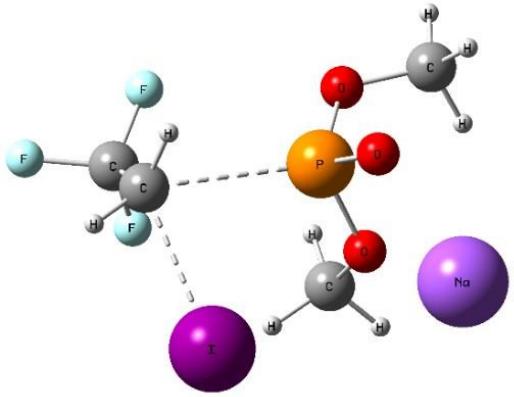

Figure 4. *TS structure for the proposed S_N2 mechanism of reaction 2. The image represents the case n=1, for n=2,3 analogously.*

The considered mechanism of the reaction is an S_N2 one, where the lone pair of the phosphorus atom is engaged in a nucleophilic attack on the carbon center linked to iodine atom. Unlike the typical mechanism for S_N2 cases, transition state (TS) eventually found by us using the QST2 method represents a side-attack approach, not a backside one (**Fig. 4**).

At first glance, the calculated differences in total reaction energy provide almost no explanation for the high discrepancies in the reactivity among the substrates. Thus, to analyze the kinetics of the reactions the free energies of activation for each system were calculated as the differences (**Eq. 4**):

$$\Delta G_n^{\ddagger} = G_{n,TS} - G_{n,COMPL}\ , \qquad (4)$$

where G_{TS} and G_{COMPL} are the values of free energy for transition state and substrate complex respectively. Next, according to the Arrhenius equation (**Eq. 5**), the kinetic rate constants k_n have been expressed as:

$$k_n = A_n \mathrm{e}^{\frac{-\Delta G_n^{\ddagger}}{RT}}, \qquad (5)$$

where k is the rate constant of considered reaction, A is an empirical value, the so-called pre-exponential factor, R – the universal gas constant and T – temperature. After a reasonable assumption of constancy of A for n = 1,2,3 in the given reaction conditions, Arrhenius equation (**Eq. 6**) may serve to designate the quotients of individual rate constants k_1, k_2 and k_3 respectively:

$$\frac{k_n}{k_i} = \mathrm{e}^{\frac{\Delta G_i^{\ddagger} - \Delta G_n^{\ddagger}}{RT}}. \qquad (6)$$

A comparison of the k_n/k_3 rate constant quotients with observed reaction yields is particularly informative (**Tab. 5**). Although all thermodynamically preferred, the individual reactions do not proceed with the same (or even similar) rate. The substrate **1c** reacts at least 2 orders of magnitude faster than **1a** and only about twice as fast as **1b**. This perfectly corresponds to the isolation yields.

Table 5. *Free energies of activation and relative rate constants of the Michaelis-Becker reaction at 273.15 K. Values in parentheses refer to 298.15 K.*

Substrate	$\Delta G^{\ddagger}$ / kcal mol^{-1}	k_n/k_3
CF_3CH_2I (**1a**)	39.48 (39.52)	0.0008 (0.0033)
$CF_3CH_2CH_2I$ (**1b**)	36.06 (36.13)	0.4175 (0.4041)
$CF_3CH_2CH_2CH_2I$ (**1c**)	35.59 (35.60)	1 (1)

To gain insight into the obtained results we studied *in silico* the Michaelis-Arbuzov reaction. For the sake of comparison, besides the fluorinated alkyl iodides (R = $CF_3(CH_2)_{n-1}$) we decided to calculate the values of thermochemical potentials (ΔH, ΔG) for the reaction of methyl iodide (R = H) which, according to the experimental results, proceeds several orders of magnitude faster.

According to the accepted S_N2-mechanism, an alkyl halide undergoes a nucleophilic attack by the phosphorus lone pair of a trivalent phosphorus ester, yielding a quaternary phosphorus salt. In the subsequent step, a nucleophilic attack of the counter anion on the alkoxy-substituent of the salt creates another alkyl halide and a dialkyl phosphonate (**Scheme 5**).

The PES stationary points for Michaelis-Arbuzov reaction, especially these corresponding to the transition state of the back-side nucleophilic attack of the phosphorus lone pair on the alkyl iodide, were obtained easily. Energetic results for the reaction path were obtained for 273.15 as well as 298.25 K (**Tab. 6**).

The listed values show that energetic outcomes for reactions 3a-b exhibit practically no temperature dependence, and their values are very close, which means that all observed discrepancies in the reaction rates should be due to kinetic factors, similarly as in the case of reaction 2.

View Article Online
DOI: 10.1039/D0NJ00963F

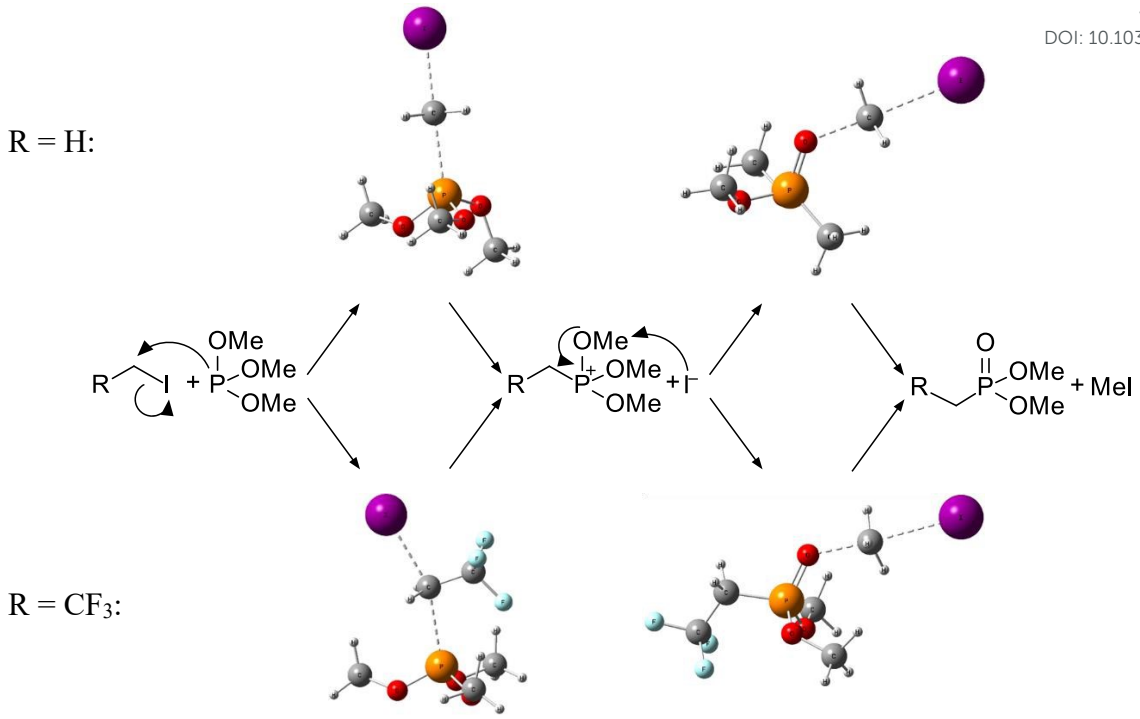

Scheme 5. *The plausible mechanism of the Michaelis-Arbuzov reaction (R = H or $CF_3(CH_2)_{n-1}$) and the calculated transition states TS1 and TS2 for two cases.*

Table 6. *Values of overall changes in thermochemical potentials for the Michaelis-Arbuzov reaction in DMF solution in temperature 273.15 K as well as 298.15 K (parentheses). All values in kcal/mol.*

Substrate	ΔH / kcal mol^{-1}	ΔG / kcal mol^{-1}
MeI	-38.59 (-38.60)	-37.32 (-37.20)
CF_3CH_2I (**1a**)	-37.69 (-37.69)	-36.21 (-36.07)
$CF_3CH_2CH_2I$ (**1b**)	-37.96 (-37.97)	-36.29 (-36.14)
$CF_3CH_2CH_2CH_2I$ (**1c**)	-36.97 (-36.98)	-34.95 (-34.77)

Two PES stationary points correspond to two transition states: TS1, connected to the nucleophilic attack of phosphorus lone pair, and TS2, connected to the attack of the counterion. Relative free energy barriers associated with them and depicted in **Tab. 6** are denoted as $\Delta G_{TS1}^{\ddagger}$ and $\Delta G_{TS2}^{\ddagger}$ respectively and calculated as:

$$\Delta G_{nTS1}^{\ddagger} = G_{n,TS1} - G_{n,COMPL}$$

for TS1 and

$$\Delta G_{n,TS2}^{\ddagger} = G_{n,TS2} - G_{n,SALT}$$

for TS2, where $G_{n,TS1}$ and $G_{n,TS2}$ are free energy values for corresponding transition states while $G_{n,COMPL}$ and $G_{n,SALT}$ are free energy values for substrate complex and quaternary salt respectively. As follows from the presented outcomes – the nucleophilic attack of the phosphorus lone pair is the rate-limiting step of the reaction considered.

View Article Online
DOI: 10.1039/D0NJ00963F

Table 7. *Energy barrier values for both transition states of Arbuzov reaction and the corresponding calculated and experimental rate constant quotients at 273.15 K. Values in parentheses refer to 298.15 K, experimental values refer to 323.15 K.*

Substrate	$\Delta G^{\ddagger}_{nTS1}$ / kcal mol^{-1}	$\Delta G^{\ddagger}_{nTS2}$ / kcal mol^{-1}	$k_n/k_{MeI;\ calc.}$		$k_n/k_{MeI;\ exper.}$
MeI	16.71 (16.91)	14.51 (14.49)	1.0	(1.0)	1.0
1a	25.26 (25.45)	14.65 (14.73)	$1.4\cdot10^{-7}$	$(5.3\cdot10^{-7})$	$2.84\cdot10^{-6}$
1b	21.85 (22.16)	13.44 (13.44)	$7.6\cdot10^{-5}$	$(1.4\cdot10^{-4})$	$3.40\cdot10^{-5}$
1c	18.02 (18.04)	13.01 (13.02)	$8.9\cdot10^{-2}$	$(1.4\cdot10^{-1})$	$3.51\cdot10^{-4}$

It is visible that the general trends observed in the experiment are closely followed by the theoretical results except for the compound **1c**. Nevertheless, in the case of **1c,** the observed discrepancy of two orders of magnitude translates to roughly 2.0 kcal/mol error in $\Delta G^{\ddagger}_{3TS1}$value – the applied level of theory permits such an error. Moreover, the longer the fluoroalkyl chain, the more conformers (*i.e.* local minima on PES) it possesses. Apparently, $G_{3,COMPL}$-minimum found by us (and used in the $\Delta G^{\ddagger}_{3TS1}$calculations) is not a global minimum but a local one that is about 2.0 kcal/mol higher in energy than the global one. The reaction rate heavily depends on the proximity of the CF_3 group. Substrate **1a** reacts about 6-7 orders of magnitude slower than MeI.

2.5. Synthesis

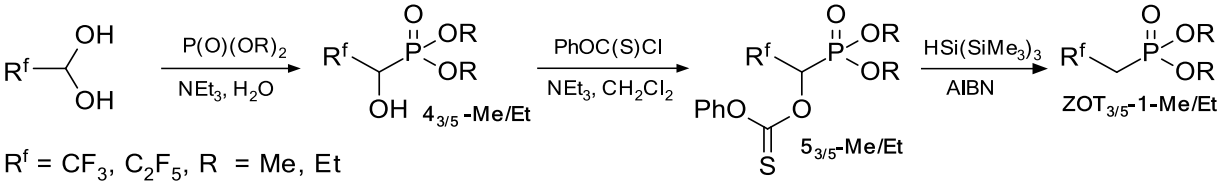

Scheme 6. *The three-step synthesis of the* ***ZOT$_{3/5}$-1*** *compounds.*

Since the Arbuzov reaction proved to be unsuccessful in the case of compounds with the shortest carbon chain we developed another strategy to synthesize the desired fluorinated phosphonates(**Scheme 6**). The protocol started from relatively cheap and readily available perfluorinated aldehyde hydrates (either fluoral hydrate or pentafluoropropionaldehyde hydrate). Upon treatment with dialkyl *H*-phosphonate in water with the aid of triethylamine, the corresponding dialkyl polyfluoroalkyl 2-hydroxyphosphonate was formed. The reaction run smoothly and large amounts of thermal energy were released. The hydroxyphosphonates were obtained as racemates. Single distillation was sufficient for purification for further steps. The hydroxyphosphonates were subsequently reacted with *O*-phenyl chlorothionoformate, yielding xanthates, which were purified by short flash chromatography.

To finally release the desired polyfluorinated phosphonates we attempted to apply standard Barton-McCombie reaction protocol with tributyltin as a hydrogen source. However, the organotin by-products were found to be virtually impossible to remove through extraction and distillation. Any attempt of chromatography led to a rapid decomposition of the product. Thus, the organotin hydride was replaced with tris(trimethylsilyl)silane. Most of the by-products were removed by dissolving the dried post-reaction residue in acetonitrile and washing with hexane

or petroleum ether (pentane gave unsatisfactory results). The crude products were purified by two subsequent distillations.

2.6. Biological activity

The encouraging ADME results for ZOTs, especially, the BBB permeability and lack of interaction with P-gp, prompted us to study their biological activity in cells derived from brain.[17, 21] We decided to screen the cytotoxic properties of ZOTs in routinely used glioblastoma U87-MG cell line. Moreover, close but nonfluorinated structural analogs of the ZOTs, dialkyl (isothiocyanatomethyl)phosphonates, were demonstrated to have antiproliferative activity against some cancer cell lines including lung (A549), breast and colon cancers.[29] To evaluate whether ZOTs show tissue specificity, apart from U87-MG cells, we studied A549 lung carcinoma (solid cancer) cells and HL-60 promyelocytic leukemia (blood cancer) cells. The normal primary human peripheral blood mononuclear cells (PBMCs) were studied to assess the safety profile of ZOTs. Standard resazurin-based cytotoxicity assay was used. This assay is based on the reduction of weakly fluorescent resazurin to highly fluorescent resorufin by mitochondrial dehydrogenases of viable cells. The intensity of fluorescence corresponds to the number of live cells in a culture.

The cytotoxicity of a similar group of compounds has not been evaluated elsewhere. Their structure containing both fluorine, which usually increases biological activity, and phosphonic moiety, which mimics carboxyl group, indicated that this group of compounds is a promising candidate to study anticancer properties. In the attempt to gain the structure-activity relationship in this group, **ZOT$_3$-1-Me**, **ZOT$_3$-1-Et**, **ZOT$_5$-1-Me**, **ZOT$_5$-1-Et**, **ZOT$_3$-2-Me**, **ZOT$_3$-3-Me** were tested.

The analysis revealed that the pentafluorinated compounds (**ZOT$_5$** group, *i.*e. **ZOT$_5$-1-Me** and **ZOT$_5$-1-Me**) but not trifluorinated compounds **ZOT$_3$** group, *i.*e. **ZOT$_3$-1-Me**, **ZOT$_3$-1-Et**, **ZOT$_3$-2-Me**, **ZOT$_3$-3-Me**) exhibited cytotoxicity toward glioblastoma, lung carcinoma and promyelocytic leukemia cells (**Fig. 5, Tab. 8**). Their cytotoxic activity depended on the cell line and the compounds were the most potent toward U-87 MG cells and the least toward HL-60 cells (**Tab. 8**). Both compounds demonstrated cytotoxicity toxicity toward PBMCs comparable to that observed in cancer cell lines tested.

Table 8. *Cytotoxicity (IC_{50} ± SEM (95%CI)) of* ***ZOT$_5$-1-Me*** *and* ***ZOT$_5$-1-Et****.*

Cell line	Tissue / Disease	Me (μM)	Et (μM)
U-87 MG	Brain / Glioblastoma astrocytoma	19.30 ± 0.01 (18.43 – 20.15)	11.74 ± 0.01 (11.13 – 12.37)
A549	Lung / Non-small-cell lung carcinoma	71.62 ± 0.03 (60.98 – 84.12)	68.66 ± 0.02 (62.86 – 74.99)
HL-60	Blood / Promyelocytic leukemia	144.9 ± 0.04 (121.0 – 173.5)	84.81 ± 0.03 (75.42 – 95.37)
PBMCs	Blood / -	66.19 ± 0.03 (58.83 – 74.46)	46.10 ± 0.06 (40.28 – 52.77)

View Article Online
DOI: 10.1039/D0NJ00963F

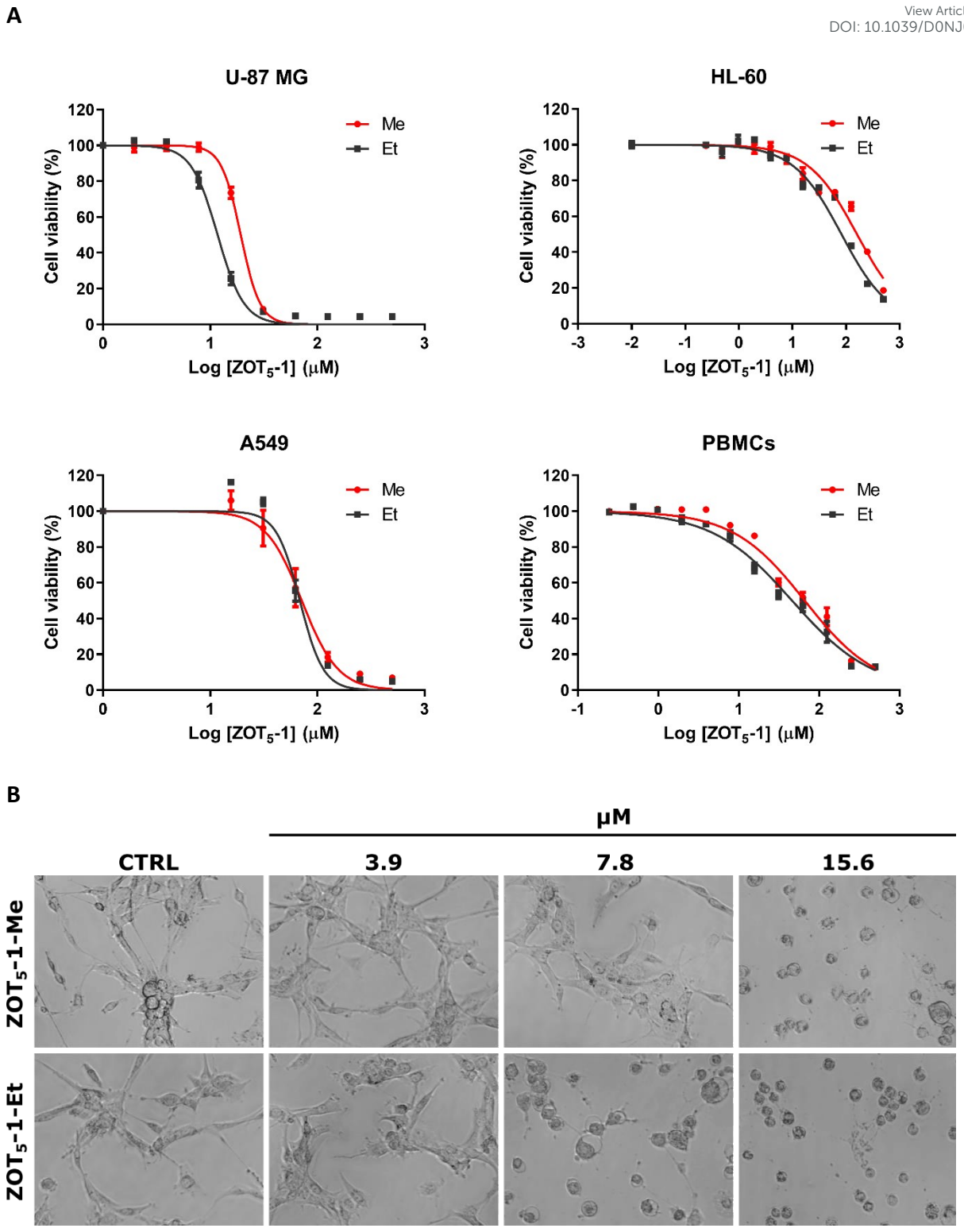

Figure 5. *The cytotoxic properties of ZOT$_5$-1-Me and ZOT$_5$-1-Et toward normal human peripheral blood mononuclear cells (PBMCs) and human cancer cells: non-small cell lung cancer cells (A549), promyelocytic leukemia cells (HL-60) and glioblastoma astrocytoma cells (U-87 MG). (**A**) Cell viability expressed as a percentage of control cells after 24 h of ZOT$_5$-1 treatment. (**B**) Changes in U-87 MG cell morphology after 24 h of ZOT$_5$-1 treatment.*

The results indicate that pentafluorinated phosphonates of this class exhibit cytotoxic properties and thus have therapeutic potential as anticancer agents. Diverse sensitivity toward cancer cells to dimethyl and diethyl derivative suggests the existence of a specific molecular target for this class of molecules. We could only speculate on its nature because cancer cell lines used in this study have different genetic constitution and origin (solid vs blood cancer). The discrepancy in the cytotoxicity between blood cells, for **ZOT$_5$-1-Me** IC_{50} values 144.9 μM for HL-60 cells and 66.19 μM for PBMCs, suggests that the insensitivity of HL-60 cells to **ZOT$_5$-1-Me** and **ZOT$_5$-1-Et** could be associated with their deficiency of p53 protein or their undifferentiated state. Dysfunction of tumor suppressor protein p53 is a common feature in the majority of human cancers since it controls apoptosis, cell cycle, and DNA repair. Therefore the mechanism of their action should further be investigated including the role of p53 and differentiation pathways. Both **ZOT$_5$-1-Me** and **ZOT$_5$-1-Et** showed to be the most effective in U-87 MG glioblastoma cells.

Since chemotherapeutics are predominantly administered intravenously, they can evoke a systemic effect of antitumor therapy. The PBMCs were used in this study for the evaluation of ZOTs cytotoxicity in primary normal cells to give an indication of possible systemic toxicity. The studied ZOTs demonstrated the cytotoxic effect towards the PBMCs, while high, was significantly lower than that observed in U87-MG cells (**ZOT$_5$-1-Me**: 66.19 μM vs 19.30 μM, $p < 0.001$ and **ZOT$_5$-1-Et**: 46.10 μM vs 11.74 μM, $p < 0.001$).

Currently, a chemotherapeutic regime for glioblastoma multiforme includes the administration of alkylating agents: temozolomide or carmustine wafer[30]. Temozolomide and carmustine show IC_{50} = 330 μM and IC_{50} = 632 μM, respectively in U-87 MG cell line after 24 h[31,32] Both **ZOT$_5$** molecules showed significantly lower cytotoxic concentration than current chemotherapeutics in U-87 MG cells after 24 h treatment, IC_{50} = 19.3 μM and IC_{50} = 11.74 μM, respectively. Temozolomide and carmustine both belong to alkylating agents, which generally are highly effective but show weakly cytotoxic properties[33].

3. Future perspectives

ZOTs constitute a new group of low molecular weight compounds combining polyfluoroalkyl and phosphonic moieties. Their unique chemical structure and simplicity hinder the prediction of the molecular mechanism of their cytotoxic properties since there is no study on biological targets of similarly structured compounds.

Although both **ZOT$_5$-1-Me** and **ZOT$_5$-1-Et** do not meet the nanomolar rule commonly considered as necessary for further preclinical studies, they demonstrated promising ADME predicted pharmacokinetic properties and constitute a new group of compounds that could be chemically modified in the purpose of increasing their cytotoxic properties. The scope of the investigated compounds could be extended in the future, especially to include longer, fully and partially fluorinated chains as well as different substituents at the phosphonic site. Therefore, we believe that this group of compounds deserves further investigation to define their molecular targets, safety, metabolism, pharmacokinetics, and pharmacodynamics. The observed toxicity toward PBMCs indicates that for the further research encapsulation before *in vivo* administration would be beneficial to lower the systemic toxicity. Simultaneously, the cytotoxic properties of ZOTs should be screen on the wide spectrum of cancer cell lines, including NCI-60 panel and glioblastoma cancer cell lines to select the most sensitive cancer types and thus reduce the off-target toxicity.

Combining the promising cytotoxic effect against the U-87 MG cell line of **ZOT$_5$-1-Me** and **ZOT$_5$-1-Et**, with the results of the ADME profiling suggesting high bioavailability of these compounds we strongly suggest further investigations of the compounds of this class.

View Article Online
DOI: 10.1039/D0NJ00963F

4. Conclusions

In silico ADME profiling predicted high bioavailability of the simplest dialkyl polyfluoroalkylphosphonates. This includes high gastrointestinal (GI) absorption and blood-brain barrier (BBB) permeability supported by non-inhibition of the main xenobiotics biotransformation executors.

Through carefully designed kinetic experiments we proved that the title compounds could not be obtained by standard Michaelis-Arbuzov or Michaelis-Becker procedures since the reactions run several orders of magnitude slower than the side reactions. We further confirmed this by *in silico* DFT calculations which agree with the experimental data up to the internal uncertainty of the theoretical method.

To overcome the problem with the availability of the compounds through an organic synthesis we developed a three-step protocol. The synthesis path starts from the addition of *H*-phosphonates to readily available perfluorinated aldehydes and follows Barton-McCombie deoxygenation, yielding the final products.

We have shown that the simplest pentafluorinated phosphonates exhibit significant toxicity towards several cancer cell lines including human non-small cell lung cancer (A549), human promyelocytic leukemia (HL-60) and human glioblastoma astrocytoma (U-87 MG). The latter cell line was found to be especially sensitive for **ZOT$_5$-1-Et** and **ZOT$_5$-1-Me**. The IC_{50} values revealed to be as low as 11.74 μM and 19.30 μM, respectively, which are lower than those of known chemotherapeutics clinically applied in the treatment of glioblastoma.

5. Acknowledgments

5.1. Financial and infrastructural support

Polish National Science Centre (Narodowe Centrum Nauki) is kindly acknowledged for providing the financial support for this research under the grant number UMO-2014/13/N/ST5/01532.

This research was supported in part by PL-Grid Infrastructure.

Dr. Emilia Obijalska (Department of Organic and Applied Chemistry, University of Lodz) is kindly acknowledged for fruitful scientific discussions and technical help. Dr. Paulina Wach (Institute of Organic Chemistry, Polish Academy of Science) is acknowledged for technical discussions.

5.2. Competitive interests

Authors have no competing interests to declare.

6. Materials and methods

6.1. Chemical syntheses

All chemicals were purchased from commercial sources and used without further purification except for solvents which were routinely distilled prior usage. Tetrahydrofuran (THF) was dried by distillation from sodium/benzophenone, dichloromethane was dried by distillation from calcium hydride.

The analytical NMR spectra were recorded on a Bruker AVANCE III 600 spectrometer in deuterated solvents. The chemical shifts (δ) are reported relative to the pre-assigned solvent peak position (for ^{1}H and $^{13}C\{^{1}H\}$) or external standard (^{19}F and $^{31}P\{^{1}H\}$).

Mass spectrometry analyses were performed as a commercial service at the Institute of Organic Chemistry, Polish Academy of Science, using Synapt G2-S mass spectrometer (Waters) equipped with the electrospray ion source and quadrupole-Time-of-flight mass analyzer. The measurement was performed in positive ion mode with the resolving power of the TOF analyzer 20000 FWHM. The exact mass measurements for all peaks were performed within 3 mDa mass error.

6.2. Kinetic experiments

Three solutions of MeI in $P(OMe)_3$ were prepared, containing 1, 2, and 4 mol% of MeI respectively. A sample of pure phosphite was used as a reference and monitored under the same conditions as well. Three separate solutions of 10 mol% of **1a**, **1b,** and **1c** respectively in $P(OMe)_3$ were made.

Each solution was placed in a capillary which was sealed by melting the tip. Each capillary was placed in an NMR tube containing 0.4 ml of D_2O. For each solution, the starting point spectra (^{1}H and ^{31}P) were registered. All tubes were placed in an oil bath at 50 °C and kept at this temperature for the duration of the experiment. Before every measurement, the NMR spectrometer was thermostated at 50 °C using a pure D_2O sample to minimize the variations of the temperature of the reaction mixtures.

The spectra were recorded on Varian GEMINI 2000 spectrometer. The spectra were taken every 2 hours for a period of the first 14 hours and then every 24 hours counting from the starting point. The longest experiment (using **1a**) took 38 days.

6.3. Synthesis

Dimethyl (2,2,2-trifluoro-1-hydroxyethyl)phosphonate (4_3-Me)

Trifluoroacetaldehyde hydrate (75% solution in water, 5 ml, 46.6 mmol) was placed in a round-bottom flask equipped with a reflux condenser at ambient temperature. Dimethyl *H*-phosphonate (10 ml, 109 mmol, 2.3 eq) was added followed by triethylamine (8 ml, 57.5 mmol, 1.25 eq). Heat release was observed. The mixture was stirred for 1 hr. Volatiles were removed on a rotary evaporator (10 mmHg, 95 °C). The residue was dissolved in water (50 ml) and extracted with diethyl ether (5×20 ml). Solvents were removed *in vacuo* to give the crude product as white crystalline solid (6.5 g, 34%) which was used without further purification. The ^{1}H, ^{31}P, and ^{19}F NMR spectra were consistent with the literature.

Colorless crystals, yield: 66.7%; mp 60-62 °C; ^{1}H NMR (600 MHz, $CDCl_3$) δ: 4.32 (dq, J = 12.7, 8.2, 1H), 3.88 (dd, J = 16.9, 10.8 Hz, 6H); ^{13}C NMR (151 MHz, $CDCl_3$) δ: 123.1 (dq, J = 281.2, 7.4 Hz), 67.6 (dq, J = 163.5, 33.7 Hz), 54.7 (d, J = 6.8 Hz), 54.0 (d, J = 7.1 Hz); ^{31}P NMR (243 MHz, $CDCl_3$) δ: 16.62 br s, ^{19}F NMR (565 MHz, $CDCl_3$) δ: -73.54 (t, J = 8.1 Hz); HR-MS (ESI) calcd for $C_4H_8F_3O_4P$ [$(M + Na)^+$]: 231.0010; found: 231.0003.

Diethyl (2,2,2-trifluoro-1-hydroxyethyl)phosphonate (4_3-Et)

Synthesized according to the procedure for **4_3-Me**.

Colorless crystals, yield: 92.9%; mp 64-65 °C; ^{1}H NMR (600 MHz, $CDCl_3$) δ: 4.34-4.23 (m, 5H), 1.39 (t, J = 7.1, 3H), ^{13}C NMR (151 MHz, $CDCl_3$) δ: 123.2 (dq, J = 280.8, 6.6 Hz), 67.7

(dq, J = 162.6, 33.3 Hz), 64.2 (dd, J = 102.3, 7.0 Hz), 16.3 (d, J = 5.7 Hz), ^{31}P NMR (243 MHz, $CDCl_3$) δ: 14.23 (q, J = 7.7 Hz), ^{19}F NMR (565 MHz, $CDCl_3$) δ: -73.30 (t, J = 8.0 Hz); HR-MS (ESI) calcd for $C_6H_{12}F_3O_4P$ [$(M + Na)^+$]: 259.0323; found: 259.0318.

Dimethyl (2,2,3,3,3-pentafluoro-1-hydroxypropyl)phosphonate (4$_5$-Me)

Synthesized according to the procedure for **4$_3$-Me**.

Colorless oil, yield: 85.0%; bp 91-93 °C at 0.40 Torr; ^{1}H NMR (600 MHz, $CDCl_3$) δ: 4.44 (ddd, J = 25.3, 13.3, 3.1 Hz, 1H), 3.88 (dd, J = 18.7, 10.9 Hz, 6H); ^{13}C NMR (151 MHz, $CDCl_3$) δ: 118.6 (qddd, J = 287.4, 37.1, 34.5, 14.1 Hz), 112.9 (ddqd, J = 261.6, 255.4, 36.9, 2.0 Hz), 66.3 (ddd, J = 162.9, 32.5, 24.9 Hz), 54.7 (d, J = 6.9 Hz), 54.0 (d, J = 7.2 Hz); ^{31}P NMR (243 MHz, $CDCl_3$) δ: 17.24; ^{19}F NMR (188 MHz, $CDCl_3$) δ: -82.84 (d, J = 3.9 Hz), -119.32 (d, J = 279.5 Hz), -127.80 (ddd, J = 279.5, 25.3, 2.8 Hz); HR-MS (ESI) calcd for $C_5H_8F_5O_4P$ [$(M + Na)^+$]: 280.9978; found: 280.9970.

Diethyl (2,2,3,3,3-pentafluoro-1-hydroxypropyl)phosphonate (4$_5$-Et)

Synthesized according to the procedure for **4$_3$-Me**.

Colorless oil, yield: 96.8%; bp 90-93 °C at 0.45 Torr; ^{1}H NMR (600 MHz, $CDCl_3$) δ: 4.41 (ddd, J = 25.0, 13.1, 2.9 Hz, 1H), 4.33-4.23 (m, 4H), 1.39 (td, J = 7.1, 2.1 Hz, 6H); ^{13}C NMR (151 MHz, $CDCl_3$) δ: 118.7 (qddd, J = 287.2, 37.2, 34.7, 13.6 Hz), 15.8 (d, J = 5.7 Hz), 113.0 (dqd, J = 145.9, 36.6, 6.4 Hz), 66.1 (ddd, J = 165.1, 31.8, 24.7 Hz), 64.0 (dd, J = 68.7, 7.1 Hz), 15.8 (d, J = 5.7 Hz); ^{31}P NMR (243 MHz, $CDCl_3$) δ: 14.78 *quasi*-t; ^{19}F NMR (188 MHz, $CDCl_3$) δ: -82.77 (d, J = 3.8 Hz), -119.04 (d, J = 279.3 Hz), -127.90 (ddd, J=279.3, 25.1, 2.8 Hz); HR-MS (ESI) calcd for $C_7H_{12}F_5O_4P$ [$(M + Na)^+$]: 309.0291; found: 309.0286.

***O*-(1-(dimethoxyphosphoryl)-2,2,2-trifluoroethyl) *O*-phenyl carbonothioate (5$_3$-Me)**

Dimethyl (2,2,2-trifluoro-1-hydroxyethyl)phosphonate (**4$_3$-Me)** (1.66 g, 8 mmol) was dissolved in CH_2Cl_2 (15 ml) and triethylamine was added (1.4 ml, 9.6 mmol, 1.2 eq). The solution was cooled in an ice-bath and *O*-phenylchlorothionoformate (1.2 ml, 8.8 mmol, 1.1 eq) was added dropwise. After the addition was completed the mixture was allowed to heat up to the rt for 30 min and stirring was continued for 1.5 hr. Water (15 ml) was added, the mixture was vigorously stirred for 10 min. The layers were separated, the water layer was extracted with CH_2Cl_2 (3×20 ml) and combined organic phases were merged and the volatiles removed on a vacuum rotary evaporator to yield yellow oil which was purified on flash chromatography to give the product as a colorless oil (2.2 g, 80%).

Colorless oil, yield: 80.5%; R_f = 0.3 (CH_2Cl_2); ^{1}H NMR (600 MHz, $CDCl_3$) δ: 7.46-7.43 (m, 2H), 7.34-7.32 (m, 1H), 7.16-7.14 (m, 2H), 6.40 (dq, J = 13.2, 7.9 Hz, 1H), 3.93 (dd, J = 12.9, 11.1 Hz, 6H); ^{13}C NMR (151 MHz, $CDCl_3$) δ: 194.0 (d, J = 6.3 Hz), 153.7, 129.7, 127.1, 121.7 (dq, J = 281.3, 5.4 Hz), 121.4, 73.7 (dq, J = 164.9, 34.5 Hz), 54.5 (dd, J = 6.3, 3.6 Hz); ^{31}P NMR (243 MHz, $CDCl_3$) δ: 10.72 (q, J = 6.6 Hz); ^{19}F NMR (565 MHz, $CDCl_3$) δ: -69.92 (t, J = 7.3 Hz); HR-MS (ESI) calcd for $C_{11}H_{12}F_3O_5PS$ [$(M + Na)^+$]: 366.9993; found: 366.9983.

***O*-(1-(diethoxyphosphoryl)-2,2,2-trifluoroethyl) *O*-phenyl carbonothioate (5$_3$-Et)**

Synthesized according to the procedure for **5$_3$-Me**.

Colorless oil, yield: 85.4%; R_f= 0.3 (CH_2Cl_2); ^{1}H NMR (600 MHz, $CDCl_3$) δ: 7.44 (dd, J = 8.4, 7.6 Hz, 2H), 7.36 – 7.31 (m, 1H), 7.14 (dd, J = 8.6, 1.0 Hz, 2H), 6.37 (dq, J = 13.2, 7.8, 1H), 4.35 – 4.24 (m, 4H), 1.40 (dt, J = 11.0, 7.1 Hz, 6H); ^{13}C NMR (151 MHz, $CDCl_3$) δ: 194.1 (d, J = 6.3 Hz), 153.7, 129.7, 127.0, 121.8 (qd, J = 281.4, 5.1 Hz), 121.4, 74.6 (q, J = 34.2 Hz), 73.5 (q, J = 34.2 Hz), 64.4 (dd, J = 6.5, 3.5 Hz), 16.3 (dd, J = 5.6, 4.6 Hz); ^{31}P NMR (243 MHz,

$CDCl_3$) δ: 8.03 (q, J = 6.3 Hz); ^{19}F NMR (565 MHz, $CDCl_3$) δ: -70.36 (t, J = 7.3 Hz); HR-MS (ESI) calcd for $C_{13}H_{16}F_3O_5PS$ [$(M + Na)^+$]: 395.0306; found: 395.0300.

_O_-(1-(dimethoxyphosphoryl)-2,2,3,3,3-pentafluoropropyl) _O_-phenyl carbonothioate (5_5-Me)

Synthesized according to the procedure for **5_3-Me**.

Colorless oil, yield: 82.9%; R_f = 0.3 (CH_2Cl_2); ^1H NMR (600 MHz, $CDCl_3$) δ: 7.50 – 7.45 (m, 2H), 7.37 (dd, J = 10.6, 4.3, 1H), 7.18 – 7.12 (m, 2H), 6.56 (ddd, J = 21.6, 13.7, 4.2 Hz, 1H), 3.96 (dd, J = 14.1, 11.1 Hz, 6H); ^{13}C NMR (151 MHz, $CDCl_3$) δ: 193.5 (d, J = 4.6 Hz), 153.7, 129.7, 127.1, 121.3, 118.2 (qddd, J = 287.6, 36.6, 34.4, 10.9 Hz), 111.3 (ddqd, J = 265.0, 256.1, 38.8, 2.0 Hz), 72.8 (dd, J = 36.1, 23.5 Hz), 71.2 (dd, J = 36.1, 23.5 Hz), 54.5 (d, J = 6.1 Hz), 54.4 (d, J = 6.7 Hz); ^{31}P NMR (243 MHz, $CDCl_3$) δ: 11.28 (t, J = 3.3 Hz); ^{19}F NMR (565 MHz, $CDCl_3$) δ: -83.35, -118.95 (dd, J = 286.3, 4.4 Hz), -122.88 (ddd, J = 286.4, 21.1, 1.9 Hz); HR-MS (ESI) calcd for $C_{12}H_{12}F_5O_5PS$ [$(M + Na)^+$]: 416.9961; found: 416.9951.

_O_-(1-(diethoxyphosphoryl)-2,2,3,3,3-pentafluoropropyl) _O_-phenyl carbonothioate (5_5-Et)

Synthesized according to the procedure for **5_3-Me**.

Colorless oil, yield: 84.4%; R_f = 0.3 (CH_2Cl_2); ^1H NMR (600 MHz, $CDCl_3$) δ: 7.50 – 7.44 (m, 2H), 7.36 (t, J = 7.5 Hz, 1H), 7.17 – 7.12 (m, 2H), 6.53 (ddd, J = 21.3, 13.7, 4.3 Hz, 1H), 4.39 – 4.27 (m, 4H), 1.43 (dt, J = 7.0, 7.0 Hz, 6H); ^{13}C NMR (151 MHz, $CDCl_3$) δ: 193.5 (d, J = 4.7 Hz), 153.5, 129.6, 126.9, 121.1, 118.2 (qddd, J = 287.4, 36.6, 34.7, 10.7 Hz), 111.2 (ddqd, J = 264.9, 256.9, 38.6, 1.6 Hz), 72.3 (ddd, J = 163.7, 35.7, 23.3 Hz), 64.3 (t, J = 6.4 Hz), 16.1 (t, J = 5.6 Hz); ^{31}P NMR (243 MHz, $CDCl_3$) δ: 8.58 (t, J = 3.3 Hz); ^{19}F NMR (565 MHz, $CDCl_3$) δ: -83.40, -118.99 (dd, J = 286.3, 4.5 Hz), -122.93 (ddd, J = 286.3, 20.9, 2.2 Hz); HR-MS (ESI) calcd for $C_{14}H_{16}F_5O_5PS$ [$(M + Na)^+$]: 445.0274; found: 445.0263.

Dimethyl (2,2,2-trifluoroethyl)phosphonate (ZOT_3-1-Me)

Xanthate **5_3-Me** (2.52 g, 6.54 mmol) was dissolved in toluene (50 ml) and the solution was heated to 80 °C. A solution of tributyltin hydride (2.2 ml, 8 mmol, 1.2 eq) and AIBN (197.0 mg, 1.25 mmol, 0.2 eq) in toluene (10 ml) was prepared at ambient temperature and added in portions to the stirred hot solution of xanthate over 30 min. The mixture was stirred until no substrate was observed on a TLC plate (around 10-20 min). The solvent was evaporated *in vacuo*. The residue was dissolved in acetonitrile (50 ml) and washed five times with hexanes. The acetonitrile layer was evaporated *in vacuo*. The product was distilled on a microdistillation apparatus twice.

Colorless oil, yield: 87.1%; bp 95-96 °C at 38 Torr; ^1H NMR (600 MHz, $CDCl_3$) δ: 3.84 (d, J = 11.3 Hz, 6H), 2.76 (dq, J = 19.6, 10.7 Hz, 2H); ^{13}C NMR (151 MHz, $CDCl_3$) δ: 123.5 (qd, J = 275.8, 3.3 Hz), 53.1 (d, J = 6.3 Hz), 32.0 (dq, J = 144.4, 31.5 Hz); ^{31}P NMR (243 MHz, $CDCl_3$) δ: 18.68 (q, J = 14.0 Hz); ^{19}F NMR (565 MHz, $CDCl_3$) δ: -58.57 (dt, J = 13.8, 10.7 Hz); HR-MS (ESI) calcd for $C_4H_8F_3O_3P$ [$(M + H)^+$]: 193.0241; found: 193.0236.

Diethyl (2,2,2-trifluoroethyl)phosphonate (ZOT_3-1-Et)

Synthesized according to the procedure for **ZOT_3-1-Me**.

Colorless oil, yield: 87.6%; bp 103-108 °C at 31 Torr; ^1H NMR (600 MHz, $CDCl_3$) δ: 4.20 (dq, J = 14.5, 7.1 Hz, 4H), 2.60 (dd, J = 38.2, 19.1 Hz, 2H), 1.36 (t, J = 7.1 Hz, 6H); ^{13}C NMR (151 MHz, $CDCl_3$) δ: 123.6 (qd, J = 275.7, 3.3 Hz), 62.8 (d, J = 6.3 Hz), 32.7 (dq, J = 144.0, 31.2 Hz), 16.2 (d, J = 6.2 Hz); ^{31}P NMR (243 MHz, $CDCl_3$) δ: 15.87 (q, J = 13.6 Hz); ^{19}F NMR (565 MHz, $CDCl_3$) δ: -58.53 (dt, J = 13.7, 10.7 Hz); HR-MS (ESI) calcd for $C_6H_{12}F_3O_3P$ [$(M + Na)^+$]: 243.0374; found: 243.0377.

View Article Online
DOI: 10.1039/D0NJ00963F

Dimethyl (2,2,3,3,3-pentafluoropropyl)phosphonate (ZOT$_5$-1-Me)

Synthesized according to the procedure for **ZOT$_3$-1-Me**.

Colorless oil, yield: 65.8%; bp 65-66 °C at 25 Torr; ^{1}H NMR (600 MHz, $CDCl_3$) δ: 3.86 (t, J = 7.6 Hz, 6H), 2.65 (q, J = 19.1 Hz, 2H); ^{13}C NMR (151 MHz, $CDCl_3$) δ: 118.5 (qtd, J = 285.7, 36.1, 13.8 Hz), 113.0 (tqd, J = 254.6, 39.1, 9.4 Hz), 53.0 (d, J = 6.3 Hz), 28.2 (dt, J = 144.3, 24.6 Hz); ^{31}P NMR (243 MHz, $CDCl_3$) δ: 19.29 (t, J = 5.6 Hz); ^{19}F NMR (565 MHz, $CDCl_3$) δ: -86.33, -112.55 (td, J = 18.6, 5.2 Hz); HR-MS (ESI) calcd for $C_5H_8F_5O_3P$ [$(M + H)^+$]: 243.0209; found: 243.0214.

Diethyl (2,2,3,3,3-pentafluoropropyl)phosphonate (ZOT$_5$-1-Et)

Synthesized according to the procedure for **ZOT$_3$-1-Me**.

Colorless oil, yield: 69.1%; bp 105-110 °C at 30 Torr; ^{1}H NMR (600 MHz, $CDCl_3$) δ: 4.20 (dq, J = 14.5, 7.1 Hz, 4H), 2.60 (dd, J = 38.2, 19.1 Hz, 2H), 1.36 (t, J = 7.1 Hz, 6H); ^{13}C NMR (151 MHz, $CDCl_3$) δ: 118.5 (dtd, J = 285.6, 36.0, 13.4 Hz), 113.1 (tqd, J = 254.4, 39.1, 9.4 Hz), 62.8 (d, J = 6.4 Hz), 29.0 (dt, J = 143.9, 24.5 Hz), 16.2 (d, J = 6.1 Hz); ^{31}P NMR (243 MHz, $CDCl_3$) δ: 16.45; ^{19}F NMR (565 MHz, $CDCl_3$) δ: -86.34, -112.63 (td, J = 18.6, 5.3 Hz); HR-MS (ESI) calcd for $C_7H_{12}F_5O_3P$ [$(M + Na)^+$]: 293.0339; found: 293.0342.

Dimethyl (3,3,3-trifluoropropyl)phosphonate (ZOT$_3$-2-Me)

Sodium hydride (7.14 mmol, 60% suspension) was added to dry DMF (9 ml) and the mixture was cooled down to 0 °C. Dimethyl *H*-phosphonate (7.14 mmol, 0.75 ml) was added. The mixture was allowed to warm to room temperature and was stirred for 1 hr. A solution of 1-iodo-4,4,4-trifluorobutane (3.59 mmol, 854 mg) in a dry DMF (4 ml) was added. The mixture was stirred for 24 hr. The DMF was removed on a rotary evaporator. The crude product was distilled twice.

Colorless oil, yield: 16.1%; bp 96-100 °C at 38 Torr; ^{1}H NMR (600 MHz, $CDCl_3$) δ: 3.78 (d, J = 10.9 Hz, 6H), 2.41-2.35 (m, 2H), 2.00-1.94 (m, 2H); ^{13}C NMR (151 MHz, $CDCl_3$) δ: 126.4 (qd, J = 276.2, 23.8 Hz), 52.8 (d, J = 6.6 Hz), 27.9 (qd, J = 31.2, 3.8 Hz), 18.1 (dd, J = 147.9, 3.1 Hz); ^{31}P NMR (243 MHz, $CDCl_3$) δ: 30.56; ^{19}F NMR (565 MHz, $CDCl_3$) δ: -67.95 (t, J = 10.2 Hz); HR-MS (ESI) calcd for $C_5H_{10}F_3O_3P$ [$(M + H)^+$]: 207.0398; found: 207.0403.

Dimethyl (4,4,4-trifluorobutyl)phosphonate

Synthesized according to the procedure for **ZOT$_3$-2-Me**.

Colorless oil, yield: 62.2%; bp 105-110 °C at 38 Torr; ^{1}H NMR (600 MHz, $CDCl_3$) δ: 3.78 (d, J = 10.8 Hz, 6H), 2.27-2.20 (m, 2H), 1.95-1.82 (m, 4H); ^{13}C NMR (151 MHz, $CDCl_3$) δ: 126.5 (dq, J = 276.4, 1.5 Hz), 33.8 (qd, J = 28.8, 14.7 Hz), 52.1 (d, J = 6.7 Hz), 23.4 (d, J = 143.1 Hz), 15.3 (dq, J = 6.9, 3.4 Hz); ^{31}P NMR (243 MHz, $CDCl_3$) δ: 32.67; ^{19}F NMR (565 MHz, $CDCl_3$) δ: -66.34 (t, J = 10.7 Hz); HR-MS (ESI) calcd for $C_6H_{12}F_3O_3P$ [$(M + Na)^+$]: 243.0374; found: 243.0373.

6.4. Theoretical calculations

The calculations were conducted using Gaussian 09 set of codes. The method used was Density Functional Theory (B3LYP functional with empirical GD3 correction for dispersion interactions: B3LYP-GD3, together with def2tzvp basis set[34] with an ECP pseudopotential[35] for the iodine atom; both adopted from EMSL Basis Set Exchange site[36]). The chosen basis set corresponds to the 6-311G(2df,p) Pople basis set.

Calculations were made for the condensed phase. The solvent (DMF) was modeled using CPCM approximation. Specific necessary solvent parameters for correct simulation were adopted from the literature[37] and Gaussian website[38] as follows:

EPS=37.219[38]
RSOLV=2.647[37]
DENSITY=0.007777[37]
VMOL=128.7[37]
EPSINF=2.039[37]

Thermochemical corrections for reagents were calculated for the temperature of 275.15 K (the creation of sodium salt) and 298.15 K (ambient reaction temperature).

All TS, as well as structures of reactant and product complexes, were confirmed by vibrational analysis to be first-order saddle points and minima respectively on the Potential Energy Surface. The vibrational scaling factor was chosen to be 0.98.

6.5. Cell line and culture

Human glioblastoma astrocytoma (U-87 MG) cell line was purchased from HPA Culture Collections and supplied by Sigma-Aldrich (Sigma-Aldrich, Poznan, Polska). Human non-small cell lung cancer (A549) cell line was obtained from American Type Culture Collection (ATCC, Rockville, MD, USA). Human promyelocytic leukemia (HL-60) was a kind gift from dr Adrianna Nowak from Lodz University of Technology. Human peripheral blood mononuclear cells (PBMCs) were isolated using Histopaque 1077 (Sigma-Aldrich, Poznań, Polska) from leukocyte buffy coat obtained from the Blood Donation Center in Lodz, Poland. U-87 MG cells were grown in EMEM (Sigma-Aldrich) with 1% non-essential amino acids (Sigma-Aldrich) and 1 mM sodium pyruvate (Sigma-Aldrich). A549 cells were cultured in DMEM:F-12 1:1 mixture medium with 15 mM HEPES (Lonza, Basel, Switzerland), HL-60 cells were maintained in IMDM medium with 15 mM HEPES (Lonza) and PBMCs were cultured in RPMI 1640 medium (Lonza). All media were supplemented with 2 mM L-glutamine (Lonza), 100 units/ml penicillin (Lonza), 100 µg/ml streptomycin (Lonza) and 10% fetal bovine serum (FBS, Biowest, Nuaillé, France), except for HL-60 cell medium which contained 15% FBS. Cells were incubated in standard conditions (37 °C, 5% CO_2, relative humidity 100%).

6.6. Cytotoxicity

Compounds cytotoxicity was determined with the resazurin-based *in vitro* toxicology assay kit (Sigma-Aldrich, Poznan, Polska). Shortly, 10 000 cancer cells or 50 000 PBMCs in 100 µl culture medium were seeded on 96-well plate a day before the experiment and then exposed in triplicate to different concentrations of compounds for 24 h. Tested compounds were prepared in DMSO and diluted in medium with the final concentration of DMSO lower than 1%. After the incubation, the resazurin dye solution was added in an amount equal to 10% of the culture medium volume, and the cells were incubated for another 3 h. Then the fluorescence intensity was measured with the excitation and emission set at 530/25 nm and 590/35 nm, respectively using a Synergy HT spectrophotometer (Biotek, Bad Friedrichshall, Germany). The cytotoxic effect was expressed as the % of negative control cells. All of the results were presented as the mean ± SEM. Calculations of IC_{50} and their 95% confidence intervals (95%CI) were conducted using GraphPad Prism 5 Software (Intuitive Software for Science, San Diego, CA).

7. Literature

1 C. Lau, S. Dagnino, K. Kato, X. Ye, A. M. Calafat, G. W. Olsen, J. L.Reiner, B. J. Place, N. Kudo, Q. Jiang, H. Gao, L. Zhang, B. D. Abbott, H.Viberg, E. Mariussen, D. E. Keil, C. E. Reed, S. E. Fenton, G. L. Kennedy, J. M. Symons, N. Khalil, M. Lee, K. Steenland, J. Wambaugh, J. L. Butenhoff, J. V. Rodricks, A. A. Rooney, A. L. Boyles, V. R. Walker, R. C. Buck, J. C. DeWitt, *Toxicological Effects of Perfluoroalkyl and Polyfluoroalkyl Substances*, Humana Press, Cham, 2019.

2 J. Wang, M. Sánchez-Roselló, J. L. Aceña, C. d. Pozo, A. E. Sorochinsky, S. Fustero V. A. Soloshonok, H. Liu, *Chem. Rev.*, 2013, **114**, 2432-2506.

3 Y. Kobayashi, I. Kumadaki, *Acc. Chem. Res.*, 1978, **11**, 197-204.

4 M. Schlosser, *Tetrahedron*, 1978, **34**, 3-17.

5 R. Filler, Y. Kobayashi, *Biomedical Aspects of Fluorine Chemistry*, Elsevier, Amsterdam, 1982.

6 J. T. Welch, *Tetrahedron*, 1987, **43**, 3123-3197.

7 G. Resnati, *Tetrahedron*, 1993, **49**, 9385-9445.

8 P. Kafarski, Phosphonates: Their Natural Occurrence and Physiological Role. In *Biological Role of Phosphorus*, IntechOpen, 2019.

9 G. Somogyi, P. Buchwald, N. Bodor, *Pharmazie*, 2002, **57**, 135-137.

10 A. Misra, S. Ganesh, A. Shahiwala, S. P. Shah, *J. Pharm. Sci.*, 2003, **6**, 252-273.

11 A. A. Kadyrov, E. M. Rokhlin, *Bull. Acad. Sci. USSR. Div. Chem. Sci.*, 1983, **32**, 1224-1230.

12 S. Hyde, J. Veliks, B. Liégault, D. Grassi, M. Taillefer, V. Gouverneur, *Angew. Chem. Int. Ed.*, 2016, 55, 3785-3789.

13 J. Zhang, X. Huang, R. K. Zhang, F. H. Arnold, *J. Am. Chem. Soc.*, 2019, **141**, 9798-9802.

14 J. Luo, E. J. Han, Q. Shen, M. Huang, Y.G. Huang, H. M. Liu, W. Wang, Q. Y. Chen, Y. Guo, *Org. Process Res. Dev.*, 2016, **20**, 1988-1992.

15 V. S. Ostrovskii, I. P. Beletskaya, I. D. Titanyuk, *Org. Lett.*, 2019, **21**, 9080-9083.

16 Bioinformatics, S. I. o. SwissADME. http://www.swissadme.ch/index.php.

17 A. Daina, O. Michielin, V. Zoete, *Scientific Reports*, 2017, **7**, 42717.

18 T. Cheng, Y. Zhao, X. Li, F. Lin, Y. Xu, X. Zhang, Y. Li, R. Wang, L. Lai, *J. Chem. Inf. Model.*, 2007, **47**, 2140-2148.

19 P. Ertl, B. Rohde, P. Selzer, *J. Med. Chem.*, 2000, **43**, 3714-3717.

20 J. S. Delaney, *J. Chem. Inf. Comput. Sci.*, 2004, **44**, 1000-1005.

21 A. Daina, V. Zoete, *ChemMedChem,* 2016, **11**, 1117-1121.

22 C. A. Lipinski, F. Lombardo, B. W. Dominy, P. J. Feeney, *Adv. Drug. Deliv. Rev.*, 2001, **46**, 3-26.

23 A. K. Ghose, V. N. Viswanadhan, J. J. Wendoloski, *J. Comb. Chem.*, 1999, **1**, 55-68.

24 D. F. Veber, S. R. Johnson, H. Y. Cheng, B. R. Smith, K. W. Ward, K. D. Kopple, *J. Med. Chem.*, 2002, **45**, 2615-2623.

25 W. J. Egan, K. M., Jr. Merz, J. J. Baldwin, *J. Med. Chem.*, 2000, **43**, 3867-3877.

26 I. Muegge, S. L. Heald, D. Brittelli, *J. Med. Chem.*, 2001, **44**, 1841-1846.

27 J. B. Baell, G. A. Holloway, *J. Med. Chem.*, 2010, **53**, 2719-2740.

28 Wolfram Research, I. Wolfram|Alpha Knowledgebase, Champaign, IL. https://www.wolframcloud.com/.

29 M. Psurski, K. Błażewska, A. Gajda, T. Gajda, J. Wietrzyk, J. Oleksyszyn, *Bioorg. Med. Chem. Lett.*, 2011, **21**, 4572-4576.

30 L. S. Ashby, K. A. Smith, B. Stea, *World J. Surg. Oncol.*, 2016, **14**, 225.

31 G. N. Castro, N. Cayado-Gutierrez, F. C. Zoppino, M. A. Fanelli, F. D. Cuello-Carrion, M. Sottile, S. B. Nadin, D. R. Ciocca, *Cell Stress Chaperones*, 2015, **20**, 253-265.
32 H. F. Chang, W. T. Huang, H. J. Chen, L. L. Yang, *Molecules*, 2010, **15**, 8953-8966.
33 C. C. Wong, K. W. Cheng, B. Rigas, *J. Pharmacol. Exp. Ther.*, 2012, **341**, 572-578.
34 F. Weigend, R. Ahlrichs, *Phys. Chem. Chem. Phys.*, 2005, **7**, 3297 – 3305.
35 K. A. Peterson, D. Figgen, E. Goll, H. Stoll, M. Dolg, *J. Chem. Phys.*, 2003, **119**, 11113-11123.
36 Basis Set Exchange (BSE). https://www.basissetexchange.org/.
37 M. Buda, *J. Solid State Electrochem.*, 2013, **17**, 3027–3037.
38 http://gaussian.com/scrf/.

DOI: 10.1039/D0NJ00963F

A table of contents entry

Experimental and computational studies on formation and biological properties of the simplest polyfluoroalkyl phosphonates

Piotr M. Zagórski, Paulina Tokarz, Bartłomiej Gostyński, Paweł Tokarz

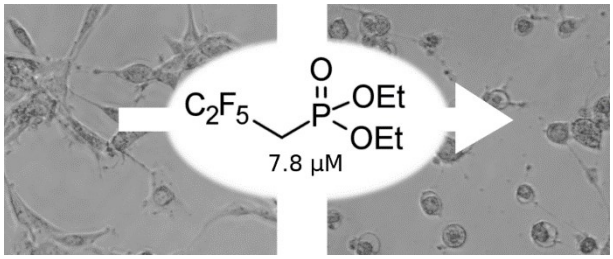

The simplest polyfluoroalkyl phosphonates exhibit high cell-line specific cytotoxicity